Molecular Identification of Immunity- and Ferroptosis-related Gene Signature in Non-small Cell Lung Cancer

Taisheng Liu
Guangzhou Medical University Affiliated Cancer Hospital
Jinye Zhang
Guangzhou Medical University Affiliated Cancer Hospital
Xiaoshan Hu
Guangzhou Medical University Affiliated Cancer Hospital
Tao Xie
Guangzhou Medical University Affiliated Cancer Hospital
Jian Zhang (zhangjian@gzhmu.edu.cn)
Guangzhou Medical University Affiliated Cancer Hospital https://orcid.org/0000-0002-0557-886X

Primary research

Keywords: lung cancer, ferroptosis, immunity, overall survival, gene signature

Posted Date: April 12th, 2021

DOI: https://doi.org/10.21203/rs.3.rs-390478/v1

Abstract

Background: Lung cancer is one of the dominant causes of cancer-related deaths worldwide. Ferroptosis, an iron-dependent regulated cell death, plays an important role in the cancer immunotherapy. However, the role of immunity- and ferroptosis-related gene signature in non-small cell lung cancer (NSCLC) remains unknown.

Method: The RNA sequencing (RNA-seq) expression data and clinical information of NSCLC were downloaded from The Cancer Genome Atlas (TCGA) database and performed differential analysis. Univariate and multivariate cox regressions were used to identify the ferroptosis-related gene, and receiver operating characteristic (ROC) model was established using the independent risk factors. GO and KEGG enrichment analyses were performed to investigate the biological functions of differential genes.

Results: A 5-gene signature was constructed to stratify patients into high- and low-risk groups. Compared with patients in the low-risk group, patients in the high-risk group showed significantly poor overall survival ($P < 0.001$ in the TCGA cohort and $P = 0.001$ in the GSE13213 cohort). The risk score was an independent predictor for overall survival in multivariate Cox regression analyses (HR > 1, $P < 0.01$). The 1 year-, 2 year- and 3 year-ROCs were 0.792, 0.644 and 0.641 in TCGA and 0.623, 0.636 and 0.631 in GSE13213, respectively. Functional analysis revealed that immune-related pathways were enriched, and immune status were different between two risk groups.

Conclusions: We identified differently expressed immunity- and ferroptosis-related genes that may involve in NSCLC. These genes may predict the overall survival in NSCLC and targeting ferroptosis may be an alternative for clinical therapy.

Background

Lung cancer has become the leading deadly malignancy worldwide (1), among which non-small cell lung cancer (NSCLC) accounts for more than 85% of all cases (2). Despite extensive research on molecular targeted therapies and checkpoint inhibitors, more than 50% of patients died within one year after diagnosis of NSCLC, and the 5-year overall survival rate is less than 18% (3). These data indicate that there is an urgent need for novel therapeutic drug research of NSCLC, and analyses of the underlying mechanism of NSCLC from a genetic level may provide clues for finding new therapeutic targets.

Ferroptosis is a type of programmed cell death associated with the imbalance of redox homeostasis (4, 5). The process of ferroptosis is usually accompanied by a large amount of iron accumulation and lipid peroxidation (6). Emerging evidence shows that ferroptosis is closely related to the development of human diseases, especially cancer (7-11) . Ferroptosis has been identified to be a promising trigger option for cancer cell death, especially for malignant tumors that are resistant to traditional therapies (12-14). Moreover, ferroptotic cancer cells might release signals like oxidized lipid mediators to affect anti-tumor immunity, or a small proportion of cells undergoing ferroptosis might suppress the immune system

and allow tumor growth (15). The induction of ferroptosis leads to the anti-tumor efficacy of immunotherapy, suggesting that the immune system might, at least in part, function through ferroptosis (16). However, the relationship between immunity- and ferroptosis-related genes and NSCLC patient prognosis is still unknown, making it still a challenge for developing ferroptosis therapy for NSCLC.

In this study, we collected the RNA-Seq data and clinical information of NSCLC in The Cancer Genome Atlas (TCGA) dataset. We identified five immunity- and ferroptosis-related differential genes to establish a prognostic risk model. Meanwhile, patients with NSCLC in the Gene Expression Omnibus (GEO) database were selected as a validation cohort. Gene Ontology (GO) and Kyoto Encyclopedia of Genes and Genomes (KEGG) analysis were used to explore the functions and pathways enriched between high-risk and low-risk subgroups. Furthermore, a nomogram model were developed based on risk scores and clinical features to assess prognosis. Our results demonstrated that the immunity- and ferroptosis-related risk model was a potential gene signature and therapeutic target for NSCLC.

Materials And Methods

Data Acquisition

The RNA sequencing (RNA-seq) data (n = 594) and corresponding clinical information of NSCLC were obtained from TCGA dataset (https://tcga-data.nci.nih.gov/tcga/). To validate the findings from TCGA dataset, we will also employ an independent cohort GSE13213 which contained 117 NSCLC cases from the GEO database (https://www.ncbi.nlm.nih.gov/geo/). The RNA-seq data and clinical information from two datasets were reviewed by two authors independently (TX-L and JY-Z) to avoid potential mistakes.

Identification of differential expression gene

The DEGs between tumor and normal tissues were identified using the “limma” R package (3.6.2 version, https://cran.r-project.org/) with the Wilcoxon test. The cut-off values were determined according to the parameters with a false discovery rate (FDR) < 0.05 and a |log2FoldChange| > 1. Univariate and multivariate cox regressions were used to evaluate the relationships between the DEGs and OS. Patients were stratified into high- and low-risk groups according to the risk score. The risk score was calculated as follow: riskscore=$\sum^{j}_{(n=1)}Coef_j*X_j$, where $Coef_j$ represents the coefficient and X_j represents the relative expression levels of each DEG standardized by z-score.

Development of ROC curves

The prognostic DEGs with clinical information was firstly analysed using the univariate cox regression. Significant prognostic factors (P< 0.05) identified by univariate cox regression were then enrolled into multivariate cox regression to identify the independent prognostic risk factors. The receiver operating

characteristic (ROC) analysis was used to determine the sensitivity and specificity of the prognostic model in predicting overall survival.

PCA and t-SNE analysis

PCA and t-SNE were used for dimensionality reduction analysis, which was applied to the gene signature using the ‘prcomp’ function in the R ‘stats’ package and the ‘Rtsne’ package, respectively. Based on the expression of genes in the signature, PCA was carried out with the "prcomp" function of the "stats" R package. Besides, t-SNE were performed to explore the distribution of different groups using the "Rtsne" R package.

Interaction network and enrichment analysis

The interaction network of DEGs was performed using the STRING database (http://string-db.org/cgi/input.pl). Moreover, GO and KEGG analysis were applied to analyze the functional enrichment of DEGs using R software (3.6.2 version, https://cran.r-project.org/).

Immune cells and ferroptosis

The infiltrating scores of 16 kinds of immune cells and the activities of 13 immune-related pathways with the ssGSEA were further evaluated using the "gsva" R package (3.6.2 version, https://cran.r-project.org/).

Statistical analysis

Statistical analysis was performed using the R software (3.6.2 version, https://cran.r-project.org/). Student's t-test was used to evaluate the difference between different groups. The ssGSEA scores between high and low-risk groups were compared by Mann–Whitney test. The Kaplan–Meier method was applied to perform OS analysis and the difference was assessed by two-sided log-rank test. Two-sided $P < 0.05$ indicated a statistically significant difference.

Results

Identification of prognostic ferroptosis-related DEGs

The workflow of our study was shown in **Fig. 1**. A total of 594 NSCLC patients from the TCGA-LUAD cohort and another 176 NSCLC patients from the GEO (GSE13213) dataset were finally enrolled. To identify ferroptosis-related differentially expressed genes (DEGs), all these samples were included for analysis while 85 samples without follow-up data were excluded for identifying ferroptosis-related genes associated with prognosis. The detailed clinical characteristics of these patients are summarized in **Table S1**. In total, we identified 16 differentially expressed genes (26.7%) between tumor and adjacent normal tissues and 14 (23.3%) prognostic genes in tumor samples (**Fig. 2A**). Notably, 5 of them (ALOX5, DPP4,

FANCD2, GCLC and SLC7A11) were both differentially expressed and correlated with overall survival (OS) in the univariate Cox regression analysis (**Fig. 2B and C**). Interaction network analysis showed that SLC7A11, GCLC, HMOX1, GCLM, G6PD, NQO1 and NOX1 were the hub genes (**Fig. 2D and E**), indicating that these genes may be the main components responsible for regulating ferroptosis in NSCLC.

Construction of a prognostic model in TCGA cohort

Based on the 5 ferroptosis-related genes (ALOX5, DPP4, FANCD2, GCLC and SLC7A11) identified above, we constructed a prognostic model using LASSO Cox regression analysis. The patients were stratified into high-risk (n = 297) and low-risk group (n = 297) groups by the median cut-off value (**Fig. 3A**). The results of principal components analysis (PCA) and t-distributed stochastic neighbor embedding (t-SNE) analysis indicated that our prognostic model could effectively stratified patients into different directions (**Fig. 3B and C**). Moreover, patients in the high-risk group had a higher probability of earlier death than those in low-risk group (**Fig. 3D**). The Kaplan-Meier curves showed that patients in the high-risk group had a significantly worse OS than their low-risk counterparts (**Fig. 3E**). Furthermore, univariate (hazard ratio [HR]: 2.97; 95% CI: 1.74–5.06; $P < 0.001$) and multivariate Cox regression analysis (HR: 2.70; 95% CI: 1.57–4.64; $P < 0.001$) also revealed that patients with high-risk achieved significantly worse OS than those with low-risk (**Table S2**). Receiver operating curve (ROC) analysis indicated that the area under the curve (AUC) of this model reached 0.792 at 1 year, 0.644 at 2 years, and 0.641 at 3 years (**Fig. 3F**). Taken together, these results suggested that the prognostic model based on the five genes had strong prognostic power.

Validation of the 5-gene signature in GSE13213 dataset

Next, we validated the prognostic model in the GSE13213 dataset. Similarly, the 107 patients were stratified into high-risk and low-risk groups by the median risk score value (**Fig. 4A**). PCA and t-SNE analysis suggested that patients with different risks were well separated into two different groups (**Fig. 4B and C**). Also, patients in the high-risk group had a higher probability of earlier death (**Fig. 4D**) and achieved significantly worse OS than those in low-risk group (**Fig. 4E**). The predictive power of our prognostic model was satisfactory (**Fig. 4F**). Furthermore, the risk score was identified as an independent predictor of OS by both univariate analysis (HR: 5.18; 95% CI: 1.8–14.92; $P < 0.01$) and multivariate Cox regression analysis (HR: 5.59; 95% CI: 1.79–17.44; $P < 0.001$; **Table S2**). Collectively, these findings suggested that our prognostic model also had strong power in GSE13213 dataset.

Functional enrichment analysis

GO enrichment and KEGG pathway analysis were performed to explore the functional roles of the DEGs in the TGCA LUAD cohort and GSE13213 dataset. GO analysis showed that the DEGs were mostly enriched in several immunity- and ferroptosis-related biological processes and molecular functions ($P < 0.05$; **Fig. 5A and B**). KEGG analysis showed that DEGs were mostly enriched in the ferroptosis pathway and immune-related pathways such as human T-cell leukemia virus 1 (HTLV-1) infection pathway ($P < 0.05$;

Fig. 5C and D). These results suggested that there may be a crosslinking between ferroptosis and tumor immune in NSCLC.

To further uncover the correlation between the risk score and immune status, the enrichment scores of diverse immune cell subpopulations and related functions or pathways with single-sample gene set enrichment analysis (ssGSEA) were further quantified. Interestingly, the antigen presentation process, including the score of aDCs, iDCs, APC co-stimulation and HLA were significantly different between the low risk and high risk group in the TCGA cohort ($P < 0.05$; **Fig. 6A and B**). APC co-inhibition and HLA class were significantly lower in high-risk patients than that in high-risk patients ($P < 0.05$; **Fig. 6B**). Comparisons in the GSE13213 dataset identified the differences of HLA class, Type I -IFN response and Type II -IFN response ($P < 0.05$; **Fig. 6C and D**). In particular, the scores of macrophages and mast cells were the most statistically different between the two risk groups in both the TCGA cohort and the GSE13213 dataset, which was consistent with the findings in the GO enrichment analysis.

Discussion

Cell death is an important aspect of mammalian development and homeostasis, which is closely associated with the physiological and pathological state of an organism (17). Ferroptosis is an iron-dependent and non-apoptotic cell death characterized by iron-dependent accumulation of lipid peroxides (18). Recent studies have suggested that ferroptosis plays an important role in cancer development and treatment (19,20). However, the immunity- and ferroptosis-related gene signature in lung cancer was still unknown. In this study, we found that 44% of ferroptosis-related genes were differentially expressed between lung tumor tissues and adjacent normal tissues, and that 5 candidate ferroptosis-related genes were significantly associated with OS. A novel prognostic model integrating 5 candidate ferroptosis-related genes was firstly constructed and validated in a GEO dataset. Functional analysis revealed that immune-related pathways were significantly enriched.

The prognostic model proposed in this study was composed of 5 ferroptosis-related genes (FANCD2, GCLC, SLC7A11, ALOX15 and DPP4). FANCD2 is a nuclear protein involved in DNA damage repair, which medicates ferroptosis in colon adenocarcinoma, clear cell renal cell carcinoma and glioma (21-23). GCLC, a glutamate-cysteine ligase catalytic subunit, acts as a glutathione-independent, non-canonical role in the protection against ferroptosis by maintaining glutamate homeostasis under cystine starvation (24-26). Inhibiting SLC7A11-mediated cystine uptake can lead to a lack of intracellular GSH and hence result in ferroptosis-mediated cell death (18,27,28). ALOX15 is closely related with lipid-ROS production in various types of tissues and tumors (29-31). DPP4, a mitochondria-encoded gene, is responsible for ferroptosis induction (26).

Functional analyses indicated that the DEGs in the high-risk and low-risk patients identified in this study were enriched in several immune-related pathways, including HTLV-1 pathway, which has been implicated in many cancers (32-35). HTLV-1 encodes two viral genes, Tax and HTLV-1 bZIP factor (HBZ), which play critical roles in viral transcription and promotion of T-cell proliferation. HBZ, a suppressor of viral

transcription, has the potential to change the immunophenotype of infected cells, conferring an effector regulatory T cell (eTreg)-like signature (CD4+ CD25+ CCR4+ TIGIT+ Foxp3+) and enhancing the proliferation of this subset (36-38). Thus, we speculate that ferroptosis may affect prognosis through HTLV-1 pathway, which drive the differentiation of Treg. Our findings also found that tumor-specific cellular immunity was altered in high-risk compared with low-risk patients. The ssGSEA score for HLA class was significantly lower in the high-risk group, indicating involve in the immune suppression.

Conclusions

Overall, our study constructed a novel immunity- and ferroptosis-related gene signature that may involve in the progression and prognosis in lung cancer. A combination of targeting both immune and ferroptosis-related genes may be a potential method for lung cancer therapy. However, the underlying mechanisms involving in tumor immunity need be further explored.

Declarations

Ethics approval and consent to participate

Not applicable.

Consent for publication

Not applicable.

Availability of data and materials

Research Data are available at TCGA.

Competing Interest

The authors declare that they have no competing interests.

Funding

This study was supported by grants from the National Natural Science Foundation of China (82003212), the Guangzhou Key Medical Discipline Construction Project Fund (02-412-B205002-1004042), Guangzhou High Level Clinical Key Specialty Construction Project (2019-2021) and Clinical Key Specialty Construction Project of Guangzhou Medical University (YYPT202017).

Author contributions

JZ and TSL performed all experiments, prepared the figures, and drafted the manuscript. TSL, TX, JYZ, and TX participated in the data analysis and results interpretation. XSH, TXL, TX, JYZ, and TX designed the study and participated in the data analysis. All authors have read and approved the manuscript.

Acknowledgements

None.

References

1. Sung H, Ferlay J, Siegel RL, Laversanne M, Soerjomataram I, Jemal A*, et al.* Global cancer statistics 2020: GLOBOCAN estimates of incidence and mortality worldwide for 36 cancers in 185 countries. *CA Cancer J Clin* (2021). doi 10.3322/caac.21660.
2. Wang L, Zhao D, Qin K, Rehman FU, Zhang X. Effect and biomarker of Nivolumab for non-small-cell lung cancer. *Biomed Pharmacother* (2019) 117:109199. doi 10.1016/j.biopha.2019.109199.
3. Borghaei H, Paz-Ares L, Horn L, Spigel DR, Steins M, Ready NE*, et al.* Nivolumab versus Docetaxel in Advanced Nonsquamous Non-Small-Cell Lung Cancer. *N Engl J Med* (2015) 373:1627-39. doi 10.1056/NEJMoa1507643.
4. Hirschhorn T, Stockwell BR. The development of the concept of ferroptosis. *Free Radic Biol Med* (2019) 133:130-43. doi 10.1016/j.freeradbiomed.2018.09.043.
5. Dixon SJ. Ferroptosis: bug or feature? *Immunol Rev* (2017) 277:150-7. doi 10.1111/imr.12533.
6. Li J, Cao F, Yin HL, Huang ZJ, Lin ZT, Mao N*, et al.* Ferroptosis: past, present and future. *Cell Death Dis* (2020) 11:88. doi 10.1038/s41419-020-2298-2.
7. Eling N, Reuter L, Hazin J, Hamacher-Brady A, Brady NR. Identification of artesunate as a specific activator of ferroptosis in pancreatic cancer cells. *Oncoscience* (2015) 2:517-32. doi 10.18632/oncoscience.160.
8. Louandre C, Marcq I, Bouhlal H, Lachaier E, Godin C, Saidak Z*, et al.* The retinoblastoma (Rb) protein regulates ferroptosis induced by sorafenib in human hepatocellular carcinoma cells. *Cancer Lett* (2015) 356:971-7. doi 10.1016/j.canlet.2014.11.014.
9. Hao S, Yu J, He W, Huang Q, Zhao Y, Liang B*, et al.* Cysteine Dioxygenase 1 Mediates Erastin-Induced Ferroptosis in Human Gastric Cancer Cells. *Neoplasia* (2017) 19:1022-32. doi 10.1016/j.neo.2017.10.005.
10. Chen MS, Wang SF, Hsu CY, Yin PH, Yeh TS, Lee HC*, et al.* CHAC1 degradation of glutathione enhances cystine-starvation-induced necroptosis and ferroptosis in human triple negative breast cancer cells via the GCN2-eIF2alpha-ATF4 pathway. *Oncotarget* (2017) 8:114588-602. doi 10.18632/oncotarget.23055.
11. Alvarez SW, Sviderskiy VO, Terzi EM, Papagiannakopoulos T, Moreira AL, Adams S*, et al.* NFS1 undergoes positive selection in lung tumours and protects cells from ferroptosis. *Nature* (2017) 551:639-43. doi 10.1038/nature24637.

12. Bebber CM, Muller F, Prieto Clemente L, Weber J, von Karstedt S. Ferroptosis in Cancer Cell Biology. *Cancers* (2020) 12. doi 10.3390/cancers12010164.
13. Liang C, Zhang X, Yang M, Dong X. Recent Progress in Ferroptosis Inducers for Cancer Therapy. *Adv Mater* (2019) 31:e1904197. doi 10.1002/adma.201904197.
14. Hassannia B, Vandenabeele P, Vanden Berghe T. Targeting Ferroptosis to Iron Out Cancer. *Cancer cell* (2019) 35:830-49. doi 10.1016/j.ccell.2019.04.002.
15. Friedmann Angeli JP, Krysko DV, Conrad M. Ferroptosis at the crossroads of cancer-acquired drug resistance and immune evasion. *Nat Rev Cancer* (2019) 19:405-14. doi 10.1038/s41568-019-0149-1.
16. Stockwell BR, Jiang X. A Physiological Function for Ferroptosis in Tumor Suppression by the Immune System. *Cell Metab* (2019) 30:14-5. doi 10.1016/j.cmet.2019.06.012.
17. Kim MJ, Yun GJ, Kim SE. Metabolic Regulation of Ferroptosis in Cancer. *Biology* (2021) 10. doi 10.3390/biology10020083.
18. Dixon SJ, Lemberg KM, Lamprecht MR, Skouta R, Zaitsev EM, Gleason CE*, et al.* Ferroptosis: an iron-dependent form of nonapoptotic cell death. *Cell* (2012) 149:1060-72. doi 10.1016/j.cell.2012.03.042.
19. Fuchs Y, Steller H. Programmed cell death in animal development and disease. *Cell* (2011) 147:742-58. doi 10.1016/j.cell.2011.10.033.
20. Thompson CB. Apoptosis in the pathogenesis and treatment of disease. *Science* (1995) 267:1456-62. doi 10.1126/science.7878464.
21. Fathima S, Sinha S, Donakonda S. Network Analysis Identifies Drug Targets and Small Molecules to Modulate Apoptosis Resistant Cancers. *Cancers* (2021) 13. doi 10.3390/cancers13040851.
22. Wu G, Wang Q, Xu Y, Li Q, Cheng L. A new survival model based on ferroptosis-related genes for prognostic prediction in clear cell renal cell carcinoma. *Aging* (2020) 12:14933-48. doi 10.18632/aging.103553.
23. Liu Y, Xu Z, Jin T, Xu K, Liu M, Xu H. Ferroptosis in Low-Grade Glioma: A New Marker for Diagnosis and Prognosis. *Med Sci Monit* (2020) 26:e921947. doi 10.12659/MSM.921947.
24. Kang YP, Mockabee-Macias A, Jiang C, Falzone A, Prieto-Farigua N, Stone E*, et al.* Non-canonical Glutamate-Cysteine Ligase Activity Protects against Ferroptosis. *Cell Metab* (2021) 33:174-89. e7 doi 10.1016/j.cmet.2020.12.007.
25. Sharma P, Shimura T, Banwait JK, Goel A. Andrographis-mediated chemosensitization through activation of ferroptosis and suppression of beta-catenin/Wnt-signaling pathways in colorectal cancer. *Carcinogenesis* (2020) 41:1385-94. doi 10.1093/carcin/bgaa090.
26. Zhang Y, Hu M, Jia W, Liu G, Zhang J, Wang B*, et al.* Hyperandrogenism and insulin resistance modulate gravid uterine and placental ferroptosis in PCOS-like rats. *J Endocrinol* (2020) 246:247-63. doi 10.1530/JOE-20-0155.
27. Stockwell BR, Friedmann Angeli JP, Bayir H, Bush AI, Conrad M, Dixon SJ*, et al.* Ferroptosis: A Regulated Cell Death Nexus Linking Metabolism, Redox Biology, and Disease. *Cell* (2017) 171:273-85. doi 10.1016/j.cell.2017.09.021.

28. Dixon SJ, Patel DN, Welsch M, Skouta R, Lee ED, Hayano M*, et al.* Pharmacological inhibition of cystine-glutamate exchange induces endoplasmic reticulum stress and ferroptosis. *eLife* (2014) 3:e02523. doi 10.7554/eLife.02523.
29. Seiler A, Schneider M, Forster H, Roth S, Wirth EK, Culmsee C*, et al.* Glutathione peroxidase 4 senses and translates oxidative stress into 12/15-lipoxygenase dependent- and AIF-mediated cell death. *Cell Metab* (2008) 8:237-48. doi 10.1016/j.cmet.2008.07.005.
30. Friedmann Angeli JP, Schneider M, Proneth B, Tyurina YY, Tyurin VA, Hammond VJ*, et al.* Inactivation of the ferroptosis regulator Gpx4 triggers acute renal failure in mice. *Nat Cell Biol* (2014) 16:1180-91. doi 10.1038/ncb3064.
31. Ou Y, Wang SJ, Li D, Chu B, Gu W. Activation of SAT1 engages polyamine metabolism with p53-mediated ferroptotic responses. *Proc Natl Acad Sci of U S A* (2016) 113:E6806-E12. doi 10.1073/pnas.1607152113.
32. He Y, Pasupala N, Zhi H, Dorjbal B, Hussain I, Shih HM*, et al.* NF-kappaB-induced R-loop accumulation and DNA damage select for nucleotide excision repair deficiencies in adult T cell leukemia. *Proc Natl Acad Sci of U S A* (2021) 118. doi 10.1073/pnas.2005568118.
33. Nosaka K, Matsuoka M. Adult T-cell leukemia-lymphoma as a viral disease: subtypes based on viral aspects. *Cancer Sci* (2021). doi 10.1111/cas.14869.
34. El Hajj H, Hleihel R, El Sabban M, Bruneau J, Zaatari G, Cheminant M*, et al.* Loss of interleukin-10 activates innate immunity to eradicate adult T cell leukemia initiating cells. *Haematologica* (2021). doi 10.3324/haematol.2020.264523.
35. Giam CZ. HTLV-1 Replication and Adult T Cell Leukemia Development. *Recent results in cancer research Fortschritte der Krebsforschung Progres dans les recherches sur le cancer* 2021;**217**:209-43 doi 10.1007/978-3-030-57362-1_10.
36. Yoshie O, Fujisawa R, Nakayama T, Harasawa H, Tago H, Izawa D*, et al.* Frequent expression of CCR4 in adult T-cell leukemia and human T-cell leukemia virus type 1-transformed T cells. *Blood* (2002) 99:1505-11. doi 10.1182/blood.v99.5.1505.
37. Karube K, Ohshima K, Tsuchiya T, Yamaguchi T, Kawano R, Suzumiya J*, et al.* Expression of FoxP3, a key molecule in CD4CD25 regulatory T cells, in adult T-cell leukaemia/lymphoma cells. *Br J Haematol* (2004) 126:81-4. doi 10.1111/j.1365-2141.2004.04999.x.
38. Yasunaga J, Sakai T, Nosaka K, Etoh K, Tamiya S, Koga S*, et al.* Impaired production of naive T lymphocytes in human T-cell leukemia virus type I-infected individuals: its implications in the immunodeficient state. *Blood* (2001) 97:3177-83. doi 10.1182/blood.v97.10.3177.

Figures

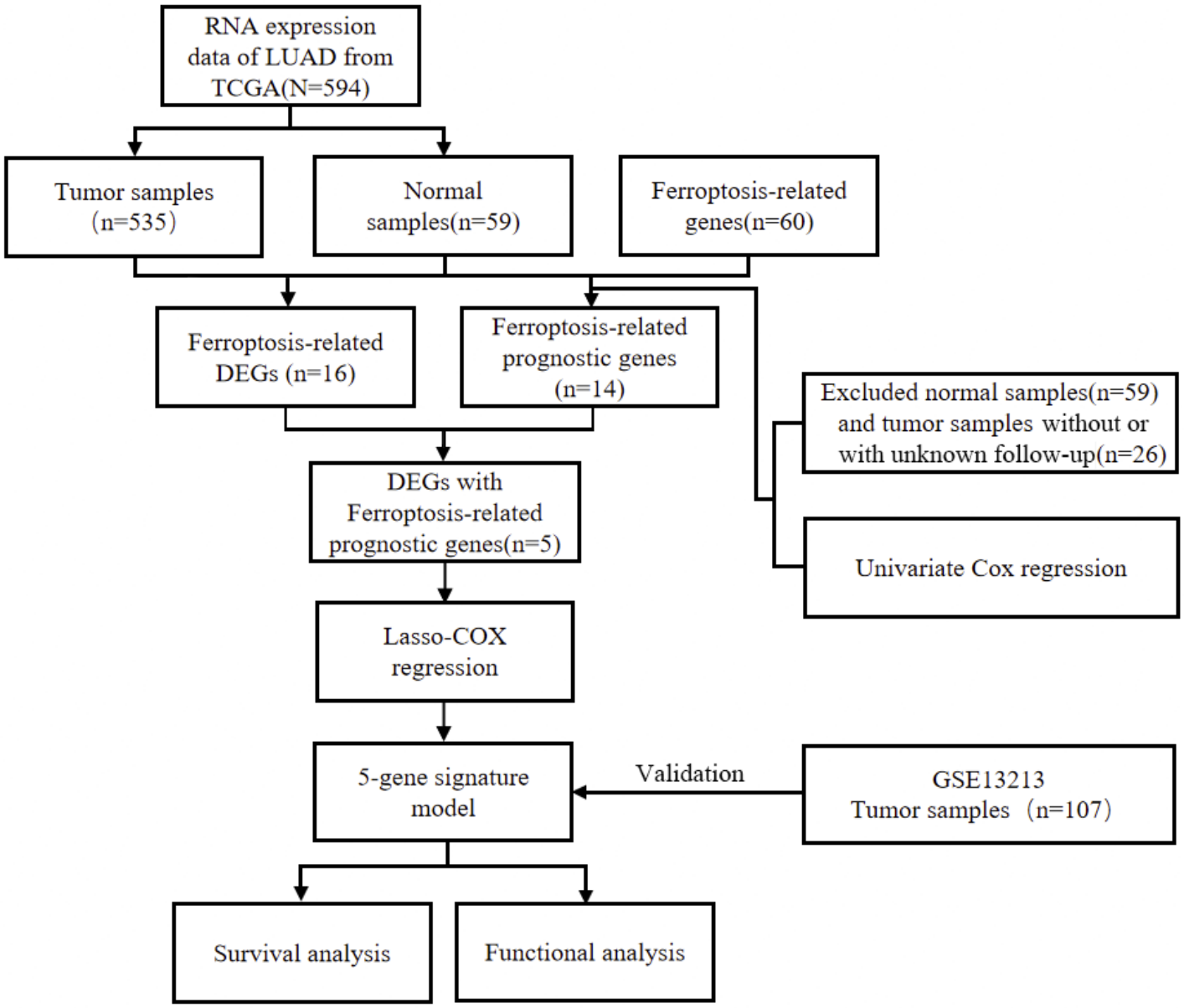

Figure 1

Flow chart of data collection and analysis.

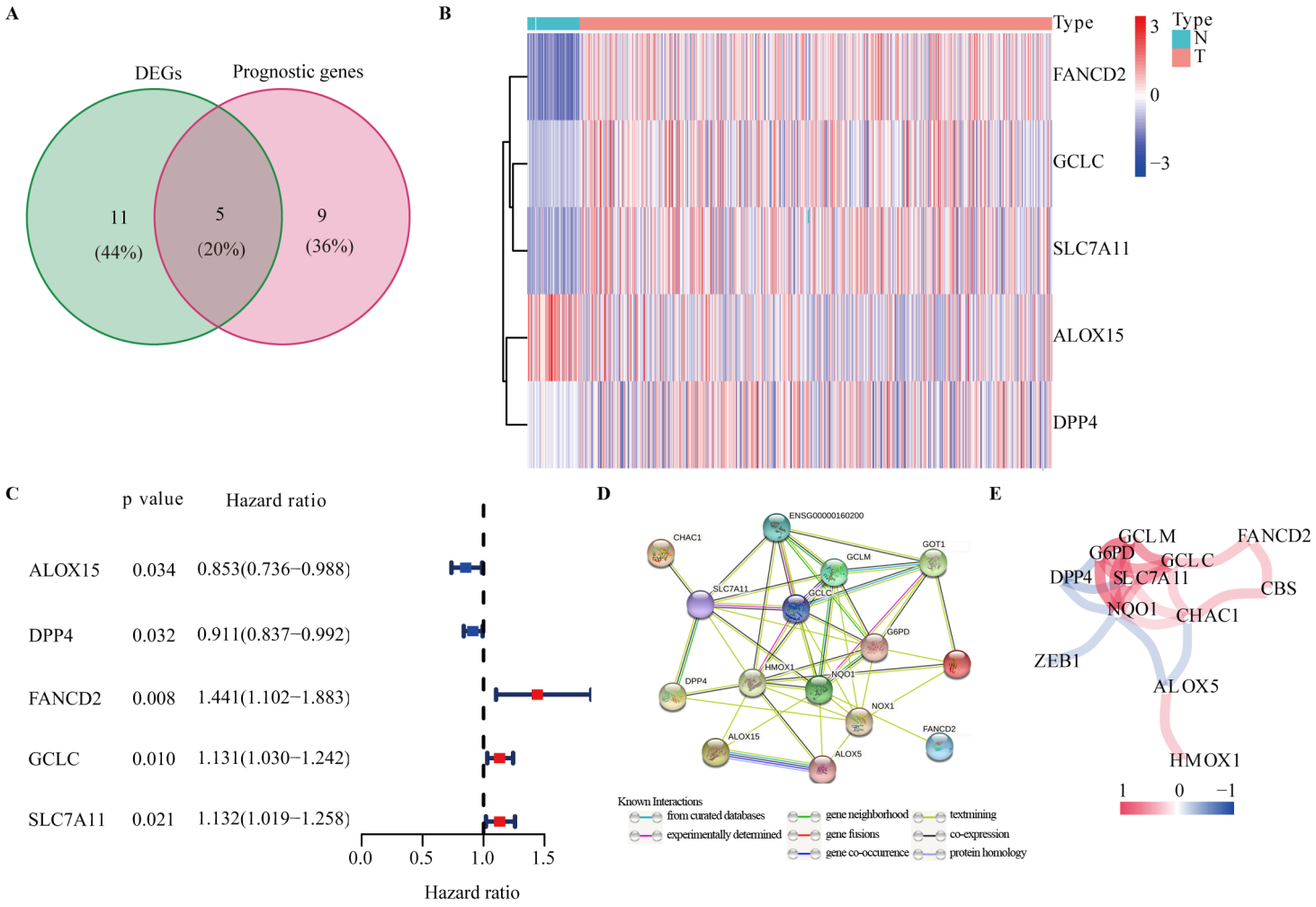

Figure 2

Identification of 5 ferroptosis-related genes in the TCGA cohort. (A) Venn diagram to identify differentially expressed genes between tumor and adjacent normal tissue that were correlated with OS. (B) The heatmap of 5 overlapping genes. (C) Forest plots showing the results of the univariate Cox regression analysis between gene expression and OS. (D) The PPI network downloaded from the STRING database indicated the interactions among the ferroptosis-related genes. (E) The correlation network of ferroptosis-related genes. The correlation coefficients are represented by different colors.

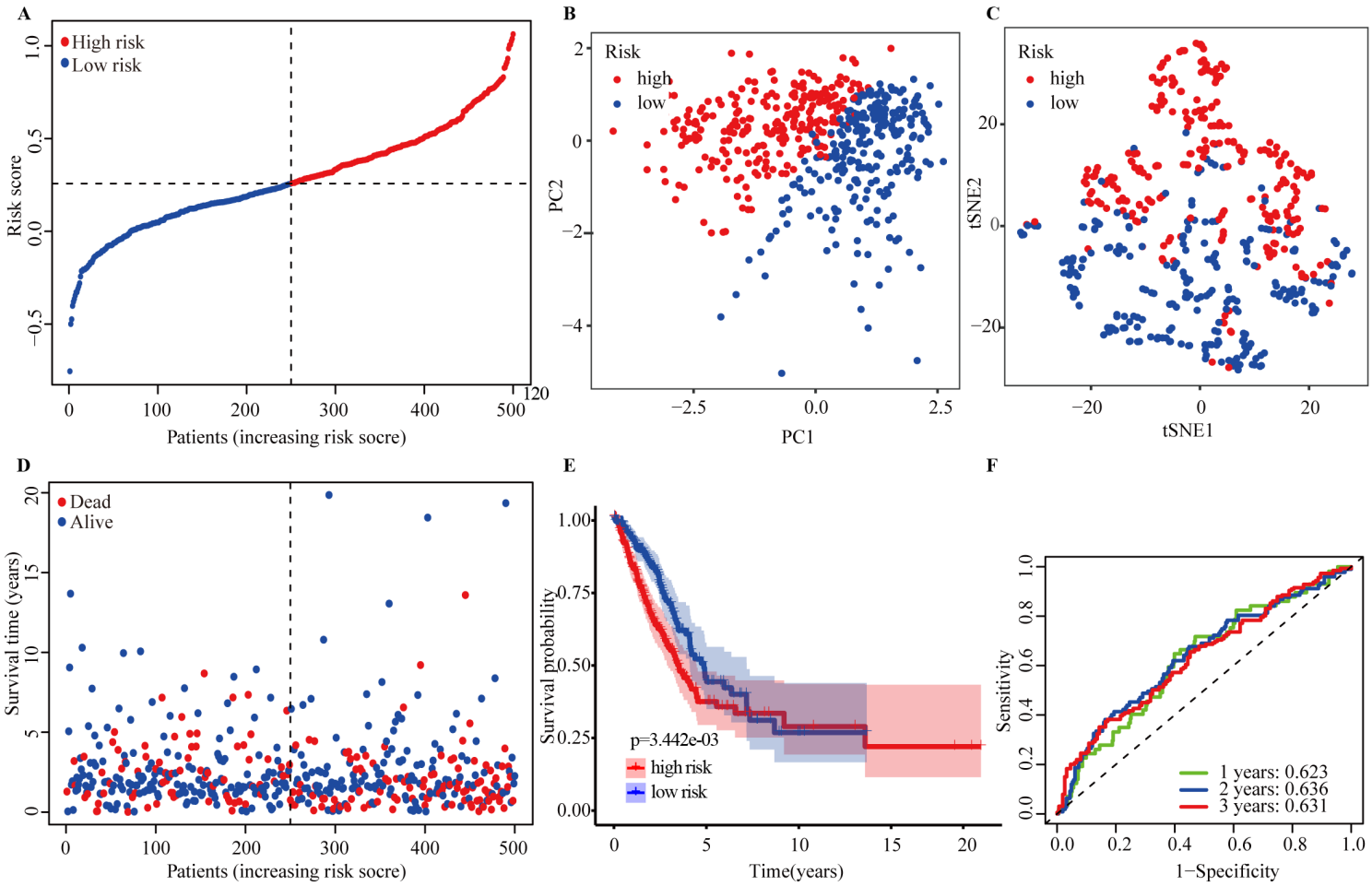

Figure 3

Prognostic analysis of the 5-gene signature model in the TCGA cohort. (A) The distribution and median value of the risk scores in the TCGA cohort. (B) PCA plot analysis of the TCGA cohort. (C) t-SNE analysis of the TCGA cohort. (D) The distributions of survival status in the TCGA cohort. (E) OS analysis of patients in the high-risk group and low-risk group in the TCGA cohort. (F) AUC of 5-gene signature model in the TCGA cohort.

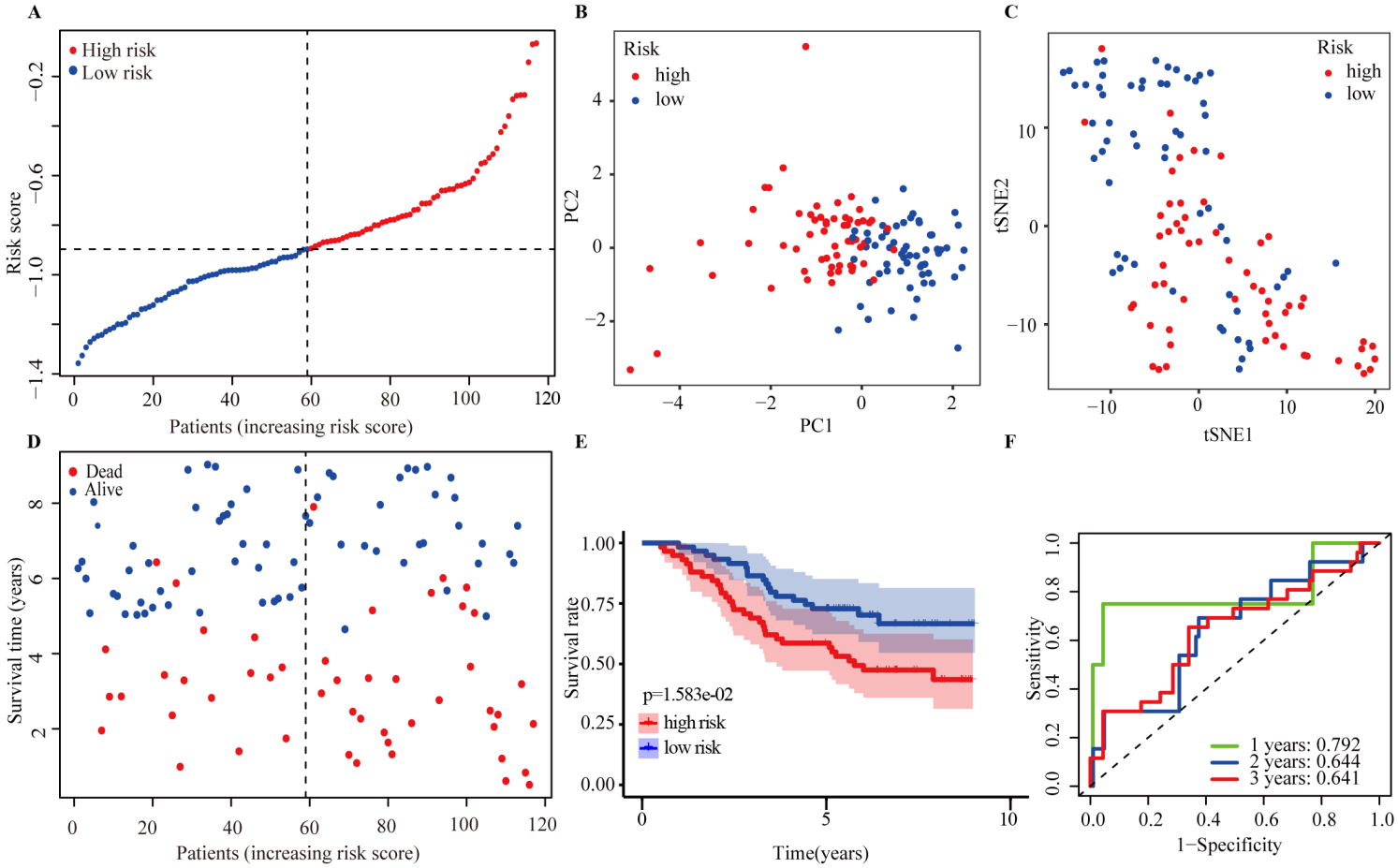

Figure 4

Validation of the 5-gene signature model in the GSE13213 dataset. (A) The distribution and median value of the risk scores in the GSE13213 dataset. (B) PCA plot analysis of the GSE13213 dataset. (C) t-SNE analysis of GSE13213 dataset. (D) The distributions of survival status in the GSE13213 dataset. (E) Kaplan-Meier OS curves between patients with high risk and low risk. (F) AUC of 5-gene signature model in the GSE13213 dataset.

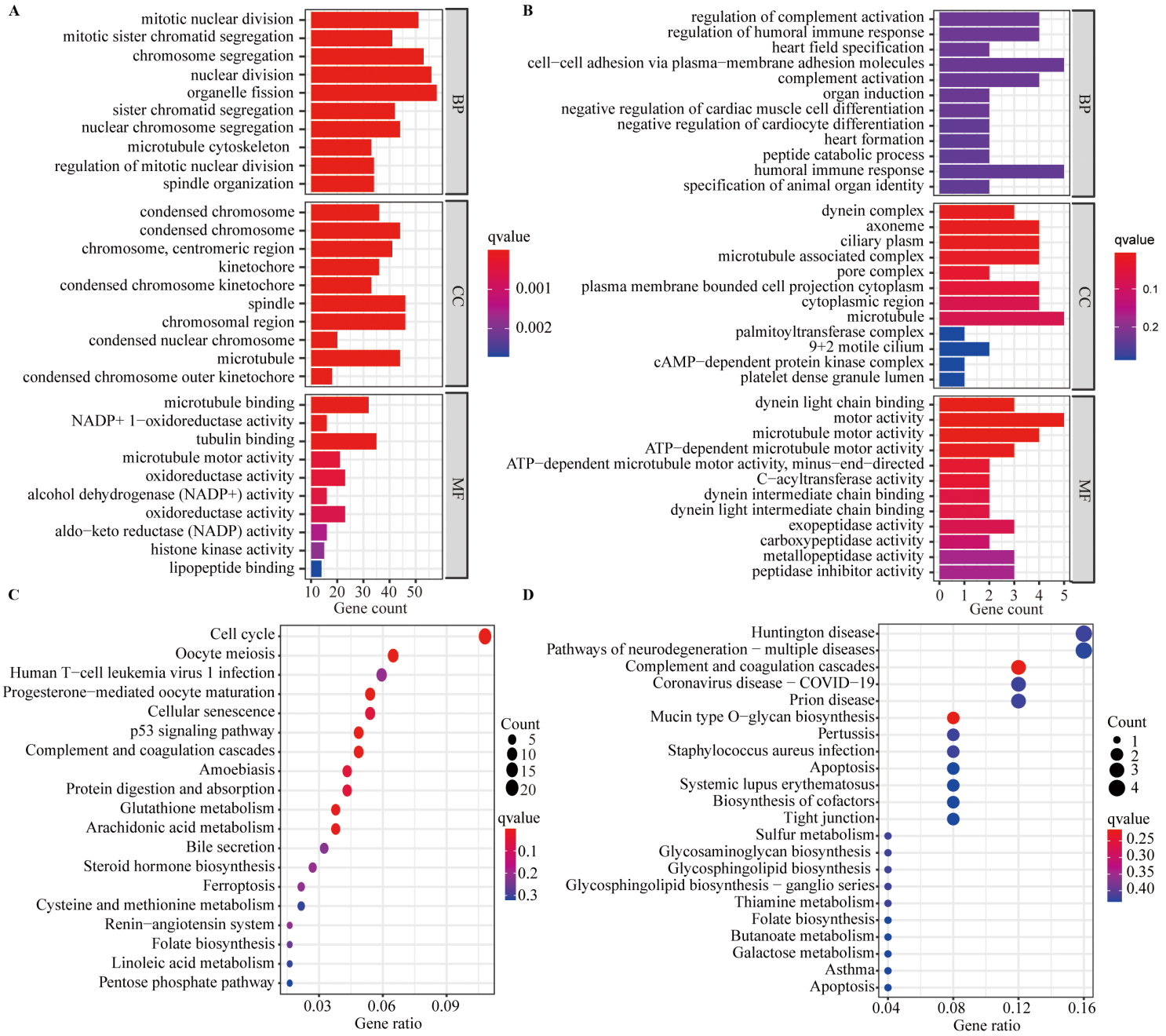

Figure 5

GO and KEGG analysis. (A-B) The most significant or shared GO enrichment in the TCGA cohort (A) and GSE13213 dataset (B) are displayed. (C-D) KEGG pathways in the TCGA cohort (C) and GSE13213 dataset (D).

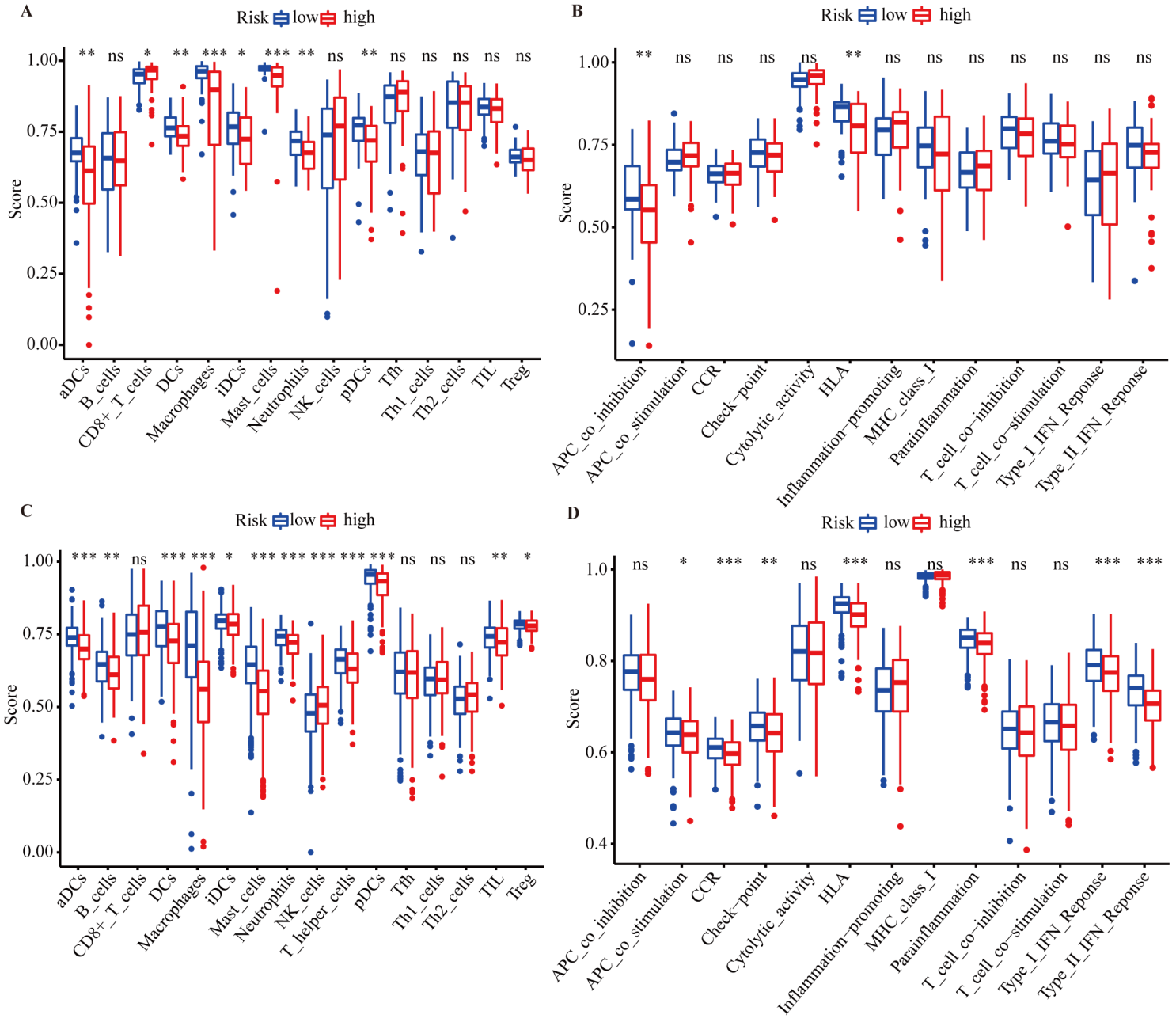

Figure 6

Comparison of the ssGSEA scores between different risk groups in the TCGA cohort and GSE13213 dataset. The scores of 16 immune cells and 13 immune-related functions are displayed in the TCGA cohort (A-B) and GSE13213 dataset (C-D). CCR, cytokine-cytokine receptor. Adjusted P values were showed as: ns, not significant; *, P< 0.05; **, P< 0.01; ***, P< 0.001.

Supplementary Files

This is a list of supplementary files associated with this preprint. Click to download.

- Table1.docx

- Table2.docx